Simulating linear covariant gauges on the lattice: a new approach

Attilio Cucchieri[*]

Instituto de Física de São Carlos, Universidade de São Paulo
Caixa Postal 369, 13560-970 São Carlos, SP, Brazil
E-mail: attilio@ifsc.usp.br

Tereza Mendes

Instituto de Física de São Carlos, Universidade de São Paulo
Caixa Postal 369, 13560-970 São Carlos, SP, Brazil
E-mail: mendes@ifsc.usp.br

Elton M. da S. Santos

Instituto de Física de São Carlos, Universidade de São Paulo
Caixa Postal 369, 13560-970 São Carlos, SP, Brazil
and
Instituto de Educação Agricultura e Ambiente, Campus Vale do Rio Madeira
Universidade Federal do Amazonas, 69800-000 Humaitá, AM, Brazil
E-mail: elton@ifsc.usp.br

We discuss a new lattice implementation of the linear covariant gauge, recently introduced in [1]. In particular, we present details of the numerical procedure for fixing the gauge. We also report on preliminary results for the transverse and longitudinal gluon propagators for the SU(2) gauge group in four space-time dimensions.

---

[*]Speaker.

1. Introduction

The infrared behavior of Green's functions in Landau gauge has been the topic of numerous lattice studies by several groups in the past few years. Particular attention has been devoted to the gluon and ghost propagators, whose infrared behavior is at the heart of the Gribov-Zwanziger confinement scenario [2, 3, 4, 5]. There is now a consistent picture — from extensive numerical simulations on very large lattices [6, 7, 8, 9, 10, 11, 12, 13, 14] — that (in three and in four space-time dimensions) the Landau gluon propagator shows a massive solution at small momenta and that the Landau ghost propagator is essentially free in the same limit. These results are not in agreement with the original Gribov-Zwanziger scenario [2, 3] but they can be explained in the so-called *refined Gribov-Zwanziger framework* [15]. Let us also recall that a massive gluon allows a better description of experimental data [16] and it has been related to color confinement by various authors [17, 18].

Since the evaluation of Green's functions depends on the gauge condition, it is important to consider different gauges in order to obtain a clear (possibly gauge-independent) picture of color confinement. Needless to say, this investigation should be carried out at the nonperturbative level. This is done from first principles using lattice simulations. In addition to the Landau gauge case cited above, numerical studies of Green's functions have also been done in Coulomb gauge [19, 20, 21], λ-gauge (a gauge that interpolates between Landau and Coulomb) [22] and maximally Abelian gauge [23, 24]. For interesting recent comparisons of results in Landau and in Coulomb gauge see [25, 26].

On the other hand, the linear covariant gauge — which is a generalization of Landau gauge — proved for a long time quite hostile to the lattice approach [27, 28, 29, 30, 31, 32, 33, 34]. Recently we have introduced a new implementation of the linear covariant gauge on the lattice [1], based on a minimizing functional that extends in a natural way the Landau case while preserving all the properties of the continuum formulation. Let us note that, having a minimizing functional for the linear covariant gauge allows a numerical investigation of the first Gribov region Ω for the case of gauge parameter $\xi \neq 0$. Such an investigation has been done analytically in [35], for a small value of ξ, but a similar numerical study is still lacking. At the same, a numerical investigation of the infrared behavior of gluon and ghost propagators at $\xi \neq 0$ could provide important inputs for analytic studies based on Dyson-Schwinger equations [36, 37]. Finally, it has been recently proven [38, 39, 40] that the background-field Feynman gauge is equivalent (to all orders) to the pinch technique [40, 41]. Thus, numerical studies using the Feynman gauge, which corresponds to the value $\xi = 1$, will allow a nonperturbative evaluation of the gauge-invariant off-shell Green's functions of the pinch technique [42].

2. Linear Covariant Gauge

In the linear covariant gauge the gluon field $A_\mu^b(x)$ satisfies (in the continuum) the relation

$$\partial_\mu A_\mu^b(x) = \Lambda^b(x)\,, \tag{2.1}$$

2

where $\Lambda^b(x)$ are real-valued functions generated using a Gaussian distribution

$$P\left[\Lambda^b(x)\right] \sim exp\left\{-\frac{1}{2\xi}\sum_b\left[\Lambda^b(x)\right]^2\right\} \tag{2.2}$$

with width $\sqrt{\xi}$.

The limit $\xi \to 0$ corresponds to the standard Landau gauge. In this case, the gauge condition is (classically) equivalent to the Lorenz-gauge (sometimes mistakenly called Lorentz-gauge) condition [43]

$$\partial_\mu A_\mu^b(x) = 0\,. \tag{2.3}$$

This condition can be imposed by minimizing the functional

$$\mathscr{E}_{LG}\{A^g\} \propto \int d^4x \sum_{\mu,b}\left[(A^g)_\mu^b(x)\right]^2 \tag{2.4}$$

with respect to the gauge transformations $\{g(x)\}$. Let us recall here that, from the second variation of $\mathscr{E}_{LG}\{A^g\}$, we can define the Faddeev-Popov operator $\mathscr{M}$. Then, for the gauge-fixed configurations, i.e. for local minima of $\mathscr{E}_{LG}\{A^g\}$, we have that this operator is positive-definite. This set of local minima defines the first Gribov region Ω [2, 3].

In Ref. [27] it was shown that a similar minimizing functional $\mathscr{E}_{LCG}\{A^g\}$ for the linear covariant gauge — i.e. for $\xi \neq 0$ — does not exist. Indeed, if it existed, we could write

$$\mathscr{E}_{LCG}[A^g,\Lambda] = \mathscr{E}_{LG}[A^g] + \mathscr{F}[A^g,\Lambda]\,, \tag{2.5}$$

for some functional $\mathscr{F}[A^g,\Lambda]$. Then, the second variation of $\mathscr{E}_{LCG}$ with respect to the gauge transformation $g(x) = e^{iw(x)}$ would satisfy the relation

$$\frac{\partial^2\mathscr{E}_{LCG}}{\partial w^b(x)\partial w^c(y)} = \frac{\partial^2\mathscr{E}_{LCG}}{\partial w^c(y)\partial w^b(x)}\,. \tag{2.6}$$

On the other hand, one can show that these two terms are, respectively, proportional to the structure functions f^{acb} and f^{abc}. Since these functions are completely anti-symmetric in the color indices, this equality cannot be realized [27].

3. Bypassing the No-Go Condition

One can of course avoid the no-go condition above by relaxing its hypotheses. For example, one can consider a different gauge condition, such as

$$F[\partial_\mu A_\mu^b(x) - \Lambda^b(x)] = 0 \tag{3.1}$$

with $F[0] = 0$, for which a minimizing functional exists. Indeed, it has been shown in Ref. [27] that the minimizing functional

$$\int d^4x \sum_{\mu,b}\left\{\left[\partial_\mu A_\mu^b(x) - \Lambda^b(x)\right]^2\right\} \tag{3.2}$$

allows one to impose the gauge condition

$$D_\nu^{ab}\partial_\nu \left[\partial_\mu A_\mu^b(x) - \Lambda^b(x)\right] = 0 \,, \tag{3.3}$$

where D_ν^{ab} is the covariant derivative.

On the other hand, the use of a different gauge condition introduces new problems [27]. For example, one can bring in spurious solutions, corresponding to $F[s] = 0$ for $s \neq 0$. In the above case, these solutions are the zeros of the operator $D_\nu^{ab}\partial_\nu$. Also, in general, the second variation of the minimizing functional, or equivalently the first variation of the gauge-fixing condition (3.1), does not correspond to the Faddeev-Popov operator $\mathcal{M} = -\partial_\mu D_\mu^{ab}$ of the usual linear covariant gauge. Finally, the lattice discretization of the functional (3.2) is not linear in the gauge transformation $\{g(x)\}$. This makes the numerical minimization difficult and one has to rely on a specific discretization of the minimizing functional [28, 29] in order to make the lattice approach feasible.

More recently [33] the no-go condition has been overcome by avoiding the use of a minimizing functional $\mathcal{E}_{LCG}\{A^g\}$. To this end, following the perturbative definition of the linear covariant gauge in the continuum, one first fixes the gluon field to Landau gauge $\partial_\mu A_\mu^b(x) = 0$. Then, one considers the equation

$$\left(\partial_\mu D_\mu^{bc}\phi^c\right)(x) = \Lambda^b(x) \,. \tag{3.4}$$

The solution $\phi^c(x)$ of this equation can be used as a generator of a second gauge transformation. Note that, after fixing the lattice (or minimal) Landau gauge, the operator $-\partial_\mu D_\mu^{bc}$ is positive-definite and can be easily inverted. For small $\phi^c(x)$, the final (gauge-transformed) gluon field $A_\mu'^b(x)$ satisfies the condition

$$\partial_\mu A_\mu'^b(x) = \partial_\mu \left(A_\mu^b + D_\mu^{bc}\phi^c\right)(x) = \Lambda^b(x) \,. \tag{3.5}$$

Of course, the above result is correct only for infinitesimal gauge transformations. On the other hand, usually $\phi^c(x)$ is not small in a numerical simulation. Indeed, numerical tests [33] have shown that the distributions of $\partial_\mu A_\mu'^b(x)$ and of $\Lambda^b(x)$ do not agree very well. At the same time, the relation $p^2 D_l(p^2) = \xi$, valid in the linear covariant gauge for the longitudinal gluon propagator $D_l(p^2)$, is also not well verified by the data at small momenta [33].

4. A New Approach

Our new approach [1] is based on removing an *implicit* hypothesis of the no-go condition, i.e. that the gauge transformation $\{g(x)\}$ appears in the minimizing functional in the "canonical" way A^g. Thus, we may look for a minimizing functional of the type $\mathcal{E}_{LCG}\{A^g, g\}$ instead of simply $\mathcal{E}_{LCG}\{A^g\}$. Indeed, the lattice linear covariant gauge condition can be obtained by minimizing the functional[1]

$$\mathcal{E}_{LCG}\{U^g, g\} = \mathcal{E}_{LG}\{U^g\} + \Re\, Tr \sum_x i\, g(x) \Lambda(x) \,, \tag{4.1}$$

where

$$\mathcal{E}_{LG}\{U^g\} = -\, \Re\, Tr \sum_{x,\mu} g(x) U_\mu(x) g^\dagger(x + e_\mu) \tag{4.2}$$

---

[1]Note that solving a system of equations $B\psi = \zeta$ is equivalent to minimizing the quadratic form $\frac{1}{2}\psi B\psi - \psi\zeta$.
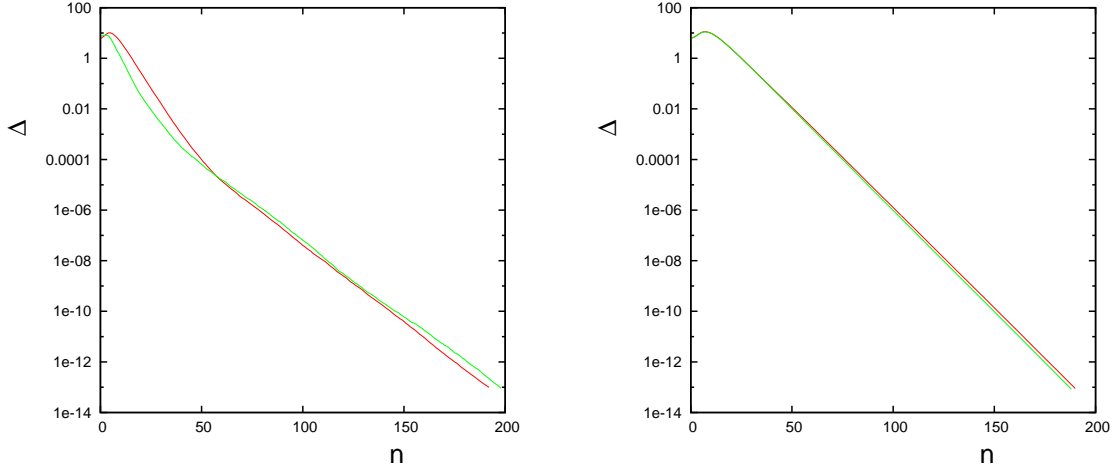
Figure 1: Convergence of the numerical gauge fixing. Here we report the value of $\Delta = \sum_{x,b}[\nabla \cdot A^b(x) - \Lambda^b(x)]^2$ as a function of the number of iterations n for a given configuration. Left: $\beta = 4$, $V = 8^4$, $\xi = 0$ (red line) and $\xi = 0.5$ (green line). Right: $\beta = 4$, $V = 16^4$, $\xi = 0$ (red line) and $\xi = 0.05$ (green line). Note the logarithmic scale on the y axis.

is the minimizing functional for the lattice Landau gauge. Here, the link variables $U_\mu(x)$ and the site variable $g(x)$ are matrices belonging to the SU(N_c) group (in the fundamental representation). We also indicate with $\Re$ the real part of a complex number and with Tr the trace in color space. Note that the functional $\mathscr{E}_{LCG}\{U^g, g\}$ is linear in the gauge transformation $\{g(x)\}$.

By considering a one-parameter subgroup $g(x, \tau) = \exp\left[i\tau\gamma^b(x)\lambda^b\right]$ of the gauge transformation $\{g(x)\}$ it is easy to check that the stationarity condition

$$\left.\frac{\partial \mathscr{E}_{LCG}}{\partial \tau}\right|_{\tau=0} = 0 \qquad \forall \ \gamma^b(x) \tag{4.3}$$

implies the lattice linear covariant gauge condition

$$\nabla \cdot A^b(x) = \sum_\mu A^b_\mu(x) - A^b_\mu(x - e_\mu) = \Lambda^b(x) . \tag{4.4}$$

Here, λ^b are the traceless Hermitian generators of the Lie algebra of the SU(N_c) gauge group, satisfying the usual normalization condition

$$Tr\left(\lambda^b \lambda^c\right) = 2\delta^{bc} . \tag{4.5}$$

Also, we used $\Lambda^b(x) = Tr[\Lambda(x)\lambda^b]$ and, similarly, $A^b_\mu(x) = Tr[A_\mu(x)\lambda^b]$.

At the same time, the second variation (with respect to the parameter τ) of the term $ig(x)\Lambda(x)$, on the r.h.s. of Eq. (4.1), is purely imaginary. Thus, it does not contribute to the second variation of the functional $\mathscr{E}_{LCG}\{U^g, g\}$. This implies that, using the above minimizing functional, one finds for the Faddeev-Popov matrix $\mathscr{M}$ a discretized version of the usual Faddeev-Popov operator $-\partial \cdot D$.

5. Numerical Tests

We have performed some numerical tests[2] with the functional (4.1), using the stochastic-overrelaxation algorithm [44, 45, 46].

For these first tests we considered the 4d SU(2) case at $\beta = 4$, for $V = 8^4$ and 16^4, with $\xi = 0.01, 0.05, 0.1$ and 0.5. The numerical gauge fixing works very well when $\xi \neq 0$, at least for relatively small lattice volumes V and gauge parameter ξ (see the next section). In Figure 1 (left panel) we compare the gauge fixing for a given configuration at $\beta = 4$ and $V = 8^4$ for the Landau case $\xi = 0$ (red line) and for $\xi = 0.5$ (green line). The rate of convergence is essentially the same in the two cases. However, note that the tuning of the stochastic-overrelaxation algorithm is different. Indeed, we found that, for the chosen configuration, the best value for the stochastic-overrelaxation parameter p was about 0.73 in the Landau case and about 0.5 when $\xi = 0.5$. A similar result (see Figure 1, right panel) is obtained for $\beta = 4$ with $V = 16^4$ for the Landau case ($\xi = 0$, red line) and for $\xi = 0.05$ (green line). In this case the best value for p was about 0.82 in the Landau case and about 0.81 when $\xi = 0.05$. Let us note that the functional $\mathscr{E}_{LCG}\{U^g, g\}$ can be interpreted as a spin-glass Hamiltonian for the *spin* variables $g(x)$ with a random interaction given by $U_\mu(x)$, in a random external magnetic field $\Lambda(x)$. The presence of this magnetic field does not modify the convergence matrix [47] or, as a consequence, the behavior of the algorithm.[3]

We also checked that the quantity $p^2 D_l(p^2)$ is constant within statistical fluctuations in all cases considered. For $V = 16^4$ and $\xi = 0.1$ and 0.5 the data are shown in Figure 2. In these cases, a fit of the type a/p^b for $D_l(p^2)$ gives $a = 0.0994(7)$, $b = 2.003(9)$ with a $\chi^2/dof = 0.9$ when $\xi = 0.1$ and $a = 0.502(5)$, $b = 2.01(1)$ with a $\chi^2/dof = 1.1$ when $\xi = 0.5$. Similar fits have been obtained in the other cases.

6. Discretization of the Gluon Field

In the above tests we used the usual discretization

$$A_\mu(x) = \frac{\left[U_\mu(x) - U_\mu^\dagger(x)\right]_{traceless}}{2i} \tag{6.1}$$

for the gluon field. However, one has to recall that, using this standard (compact) discretization, the gluon field is bounded. On the other hand, the functions $\Lambda^b(x)$ [see Eqs. (2.1) and (2.2)] satisfy a Gaussian distribution, i.e. they are unbounded. This can give rise to convergence problems [49]. Moreover, the problem is more severe for a larger width of the Gaussian distribution.

A possible way out of this problem is, of course, the use of different discretizations of the gluon field $A_\mu(x)$, in order to improve the convergence of the minimizing algorithms. To this end we also did some tests using the *angle* projection [50] and the stereographic projection [51]. Note that, in the last case, the gluon field is in principle unbounded even for a finite lattice spacing. We

---

[2]Note that Eq. (4.4) implies $\sum_x \Lambda^b(x) = 0$. Thus, after generating the functions $\Lambda^b(x)$ using the Gaussian distribution (2.2), one has to remove possible zero modes from them.

[3]Note that, in the case $\beta = \infty$ [46], the Landau case corresponds to solving the Laplace equation while the linear covariant gauge corresponds to solving a Poisson equation. As is well-known, these two equations show the same critical behavior when solved using a relaxation method such as Gauss-Seidel [48].
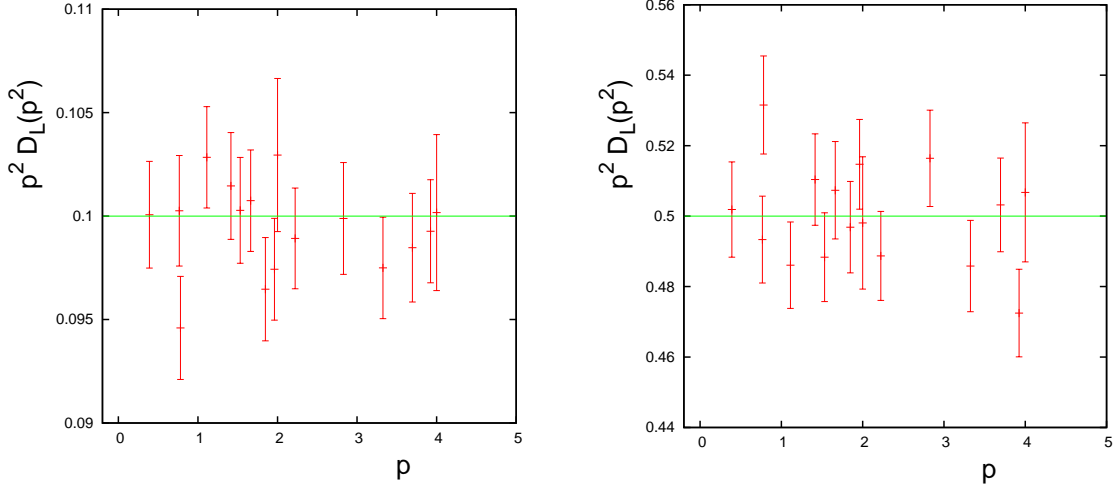
Figure 2: The longitudinal gluon dressing function $p^2 D_l(p^2)$ as a function of the lattice momentum p (in lattice units). We also show the predicted value $p^2 D_l(p^2) = \xi$. Left: $\beta = 4$, $V = 16^4$ and $\xi = 0.1$. Right: $\beta = 4$, $V = 16^4$ and $\xi = 0.5$. Note the relatively small range of values on the y axis.

Table 1: Smallest value of β for which the numerical gauge-fixing algorithm showed convergence for the lattice volume $V = 8^4$. Results are reported for the three different discretizations considered and for five different values of the gauge parameter ξ. For each case we used five different configurations.

ξ	stand. disc.	angle proj.	stereog. proj.
0.01	2.2	2.2	2.2
0.05	2.2	2.2	2.2
0.1	2.2	2.2	2.2
0.5	2.8	2.6	2.5
1.0	—	3.0	2.5

also stress that, in both cases, the numerical implementation gets simplified if one uses the Cornell method [44, 45, 46] instead of the stochastic-overrelaxation algorithm, as done in the simulations reported in the previous section.

We tested the standard discretization, the angle projection and the stereographic projection using $V = 8^4$, $\xi = 0.01, 0.05, 0.1, 0.5, 1.0$ and $\beta = 2.2, 2.3, \ldots, 2.9, 3.0$. We found (see Table 1) that the stereographic projection allows one to simulate at slightly larger values of ξ, for a given lattice volume V and lattice coupling β, compared to the other two cases.[4]

7. Continuum Limit

In Ref. [33] it was shown that in the $SU(N_c)$ case, in order to obtain the correct continuum limit, the functions $\Lambda^b(x)$ should be generated using a Gaussian distribution with width $\sqrt{\sigma} = \sqrt{2N_c \xi / \beta}$,

---

[4]Note that, as explained in the next section, the Gaussian distribution generated in the simulation actually has squared width $\sigma = 4\xi / \beta$ [in the SU(2) case].

instead of the width $\sqrt{\xi}$. Thus, for $\beta < 2N_c$ the lattice width $\sqrt{\sigma}$ is even larger than the continuum width $\sqrt{\xi}$. On the other hand, one can always obtain a sufficiently small value for σ by considering large enough values of the lattice coupling β. However, if β is too large, the physical volume is too small (for a given lattice size) and one cannot study the infrared limit of the theory.

Note that, in the SU(2) case, one has $\sigma = \xi$ only for $\beta = 4$, which corresponds to a very small lattice spacing, i.e. $a \approx 0.001$ fm [52]. On the contrary, in the SU3 case, one has $\sigma = \xi$ for $\beta = 6$, corresponding to a lattice spacing $a = 0.102$ fm [53], usually employed in lattice numerical studies. Thus, simulations for the linear covariant gauge are probably easier in the SU(3) case.

One should also recall that the gluon field A and the gauge parameter ξ are (multiplicatively) renormalized by the same factor Z_3, i.e. $A_B = Z_3^{1/2} A_R$ and $\xi_B = Z_3 \xi_R$. Here, B and R indicate bare and renormalized quantities respectively. This implies that, on the lattice, data obtained for two different values of β in the scaling region — e.g. β_1 and β_2 — would give the same (renormalized) propagator only if the multiplicative factor $R_Z = Z_3(\beta_1)/Z_3(\beta_2)$ relating the propagators[5] also relates the gauge parameters ξ_1 and ξ_2. Since the value of R_Z is not known a priori, one has to find numerically pairs of parameters (β, ξ) yielding the same continuum renormalized propagators.

8. Transverse Gluon Propagator

In this section we present preliminary results for the momentum-space transverse gluon propagator $D_t(p^2)$ for different values of ξ. Using the stereographic projection, we have simulated the linear covariant gauge at $\beta = 2.2$ and $\beta = 2.3$ for the lattice volumes $V = 8^4, 16^4$ and 24^4, considering several values of the gauge parameter ξ in the SU(2) case (see Table 2). We observe that the quantity $D_l(p^2)p^2/\xi$, which should be equal to 1, has a value of 0.999(2) when averaged over all data $D_l(p^2)$ produced. From the results shown in Figures 3 and 4 one clearly sees that, as in Landau gauge, the propagator is more infrared suppressed when the lattice volume increases. At the same time, for a fixed volume V, the propagator is also more infrared suppressed when the gauge parameter ξ increases. The latter result is in agreement with Ref. [31].

Let us recall that, on the lattice, the finite size of the system corresponds to an infrared cutoff $\sim 2\pi/L$, where L is the lattice size. In the four-dimensional case for $\beta = 2.2$, in Landau gauge, one needs to use a lattice volume V of about 64^4 in order to obtain infinite-volume-limit results [9, 10]. The data shown in Figures 3 and 4 seem to indicate that similar lattice volumes are also needed for the linear covariant gauge. On the other hand, considering the data reported in Section 6, the extrapolation to infinite volume for a given β and a fixed value of ξ seems harder than in Landau gauge. Indeed, as $V \to \infty$, the number of sites characterized by a large value for the function $\Lambda^b(x)$ increases, making the convergence of the gauge-fixing method more difficult.

9. Conclusions

We have discussed a new lattice implementation of the linear covariant gauge. The gauge fixing is done using a minimizing functional $\mathscr{E}_{LCG}\{U^g, g\}$, which is a simple generalization of the Landau-gauge functional $\mathscr{E}_{LG}\{U^g\}$. Tests done for the SU(2) case in four space-time dimensions

---

[5]See Ref. [54] for the case of Landau gauge.

Table 2: Values of the lattice coupling β, the lattice volume V and the gauge parameter ξ used in our simulations. We also report, in each case, the total number of configurations considered.

β	V	ξ	number of conf.	β	V	ξ	number of conf.
2.2	8^4	0.0	500	2.3	8^4	0.0	500
2.2	8^4	0.01	500	2.3	8^4	0.01	500
2.2	8^4	0.05	500	2.3	8^4	0.05	500
2.2	8^4	0.1	500	2.3	8^4	0.1	500
2.2	8^4	0.2	500	2.3	8^4	0.3	500
2.2	8^4	0.3	500	2.3	8^4	0.5	500
2.2	8^4	0.4	500	2.3	8^4	0.6	500
2.2	8^4	0.5	542	2.3	8^4	0.7	543
2.2	16^4	0.0	400	2.3	16^4	0.0	400
2.2	16^4	0.01	400	2.3	16^4	0.01	400
2.2	16^4	0.05	400	2.3	16^4	0.05	400
2.2	16^4	0.1	400	2.3	16^4	0.1	400
				2.3	16^4	0.2	336
2.2	24^4	0.0	158	2.3	24^4	0.0	200
2.2	24^4	0.01	200	2.3	24^4	0.01	200
2.2	24^4	0.05	160	2.3	24^4	0.05	310
				2.3	24^4	0.07	59

show that this approach solves most problems encountered in earlier implementations and ensures a good quality for the gauge fixing with a ratio $D_l(p^2)p^2/\xi \approx 1$ for all cases considered. We have also presented preliminary results for the transverse gluon propagator $D_t(p^2)$.

As discussed in Sections 6 and 8, the only open problem is the convergence of the gauge-fixing algorithm at large lattice volumes when the gauge parameter ξ is also large. However, as mentioned above, this problem is probably less severe for the SU(3) group compared to the SU(2) case. We are currently simulating other values of β and ξ in the 4d SU(2) case and considering simulations also of the SU(3) group and of the 3d case [55].

Acknowledgement

References

[1] A. Cucchieri, T. Mendes and E.M.S. Santos, Phys. Rev. Lett. **103**, 141602 (2009).

[2] V.N. Gribov, Nucl. Phys. B **139**, 1 (1978).
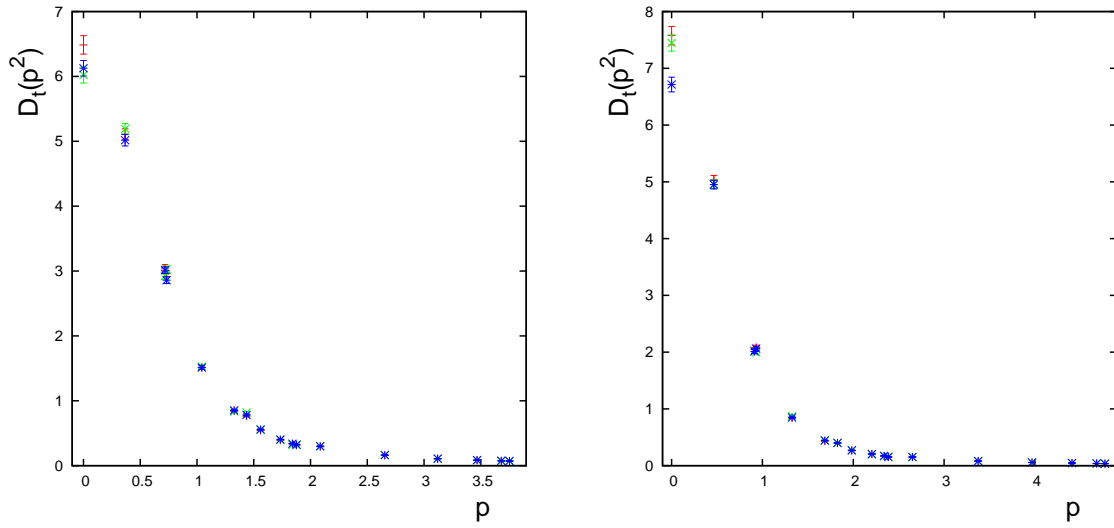
[3] D. Zwanziger, Nucl. Phys. B **412**, 657 (1994).

Figure 3: Transverse gluon propagator $D_t(p^2)$ as a function of the momentum p (both in physical units) for the lattice volume $V = 16^4$, $\beta = 2.2$ (left) and $\beta = 2.3$ (right), with $\xi = 0\,(+, red), 0.05\,(\times, green)$ and $0.1\,(\ast, blue)$.
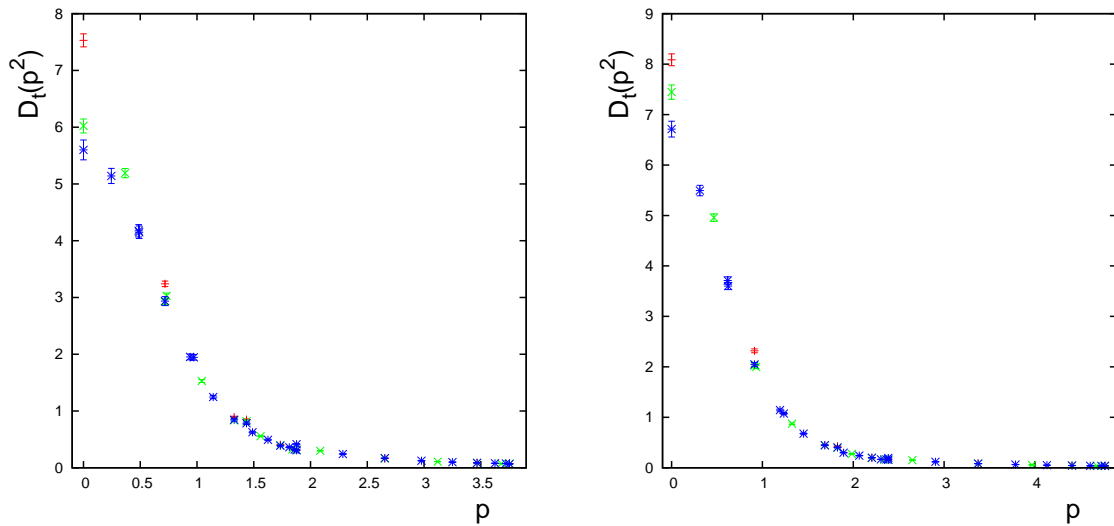

Figure 4: Transverse gluon propagator $D_t(p^2)$ as a function of the momentum p (both in physical units) for the gauge coupling $\xi = 0.05$, $\beta = 2.2$ (left) and $\beta = 2.3$ (right), with the lattice volumes $V = 8^4\,(+, red), 16^4\,(\times, green)$ and $24^4\,(\ast, blue)$.

[4] D. Zwanziger, arXiv:0904.2380 [hep-th].

[5] For a recent review see A. Cucchieri and T. Mendes, arXiv:0809.2777 [hep-lat].

[6] I.L. Bogolubsky *et al.*, PoS **LAT2007**, 290 (2007).

[7] A. Cucchieri and T. Mendes, PoS **LAT2007**, 297 (2007).

[8] A. Sternbeck *et al.*, PoS **LAT2007**, 340 (2007).

[9] A. Cucchieri and T. Mendes, Phys. Rev. Lett. **100**, 241601 (2008).

[10] A. Cucchieri and T. Mendes, Phys. Rev. D **78**, 094503 (2008).

[11] V.G. Bornyakov, V.K. Mitrjushkin and M. Muller-Preussker, Phys. Rev. D **79**, 074504 (2009).

[12] I.L. Bogolubsky *et al.*, Phys. Lett. B **676**, 69 (2009).

[13] O. Oliveira and P.J. Silva, Eur. Phys. J. C **62**, 525 (2009).

[14] M. Gong *et al.*, Mod. Phys. Lett. A **24**, 1925 (2009).

[15] D. Dudal *et al.*, arXiv:0911.0082 [hep-th], these proceedings.

[16] A.A. Natale, arXiv:0910.5689 [hep-ph], these proceedings.

[17] J.M. Cornwall, Nucl. Phys. B **157**, 392 (1979).

[18] M. Chaichian and K. Nishijima, Eur. Phys. J. C **47**, 737 (2006).

[19] For a review see e.g. A. Cucchieri, AIP Conf. Proc. **892**, 22 (2007).

[20] G. Burgio, M. Quandt and H. Reinhardt, Phys. Rev. Lett. **102**, 032002 (2009).

[21] J. Greensite, Phys. Rev. D **80**, 045003 (2009).

[22] A. Cucchieri, A. Maas and T. Mendes, Mod. Phys. Lett. A **22**, 2429 (2007).

[23] V.G. Bornyakov *et al.*, Phys. Lett. B **559**, 214 (2003).

[24] T. Mendes, A. Cucchieri and A. Mihara, AIP Conf. Proc. **892**, 203 (2007).

[25] J. Greensite, arXiv:0911.1381 [hep-lat], these proceedings.

[26] G. Burgio, M. Quandt and H. Reinhardt, arXiv:0911.5101 [hep-lat].

[27] L. Giusti, Nucl. Phys. B **498**, 331 (1997).

[28] L. Giusti *et al.*, Nucl. Phys. Proc. Suppl. **83**, 819 (2000).

[29] L. Giusti *et al.*, Phys. Rev. D **63**, 014501 (2001).

[30] L. Giusti *et al.*, arXiv:hep-lat/9912036.

[31] L. Giusti *et al.*, Nucl. Phys. Proc. Suppl. **94**, 805 (2001).

[32] L. Giusti *et al.*, Nucl. Phys. Proc. Suppl. **106-107**, 995 (2002).

[33] A. Cucchieri, A. Maas and T. Mendes, Comput. Phys. Commun. **180**, 215 (2009).

[34] T. Mendes, A. Cucchieri, A. Maas and A. Mihara, arXiv:0809.3741 [hep-lat].

[35] R.F. Sobreiro and S.P. Sorella, JHEP **0506**, 054 (2005).

[36] R. Alkofer *et al.*, Phys. Rev. D **68**, 045003 (2003).

[37] A.C. Aguilar and J. Papavassiliou, Phys. Rev. D **77**, 125022 (2008).

[38] D. Binosi and J. Papavassiliou, Phys. Rev. D **66**, 111901 (2002).

[39] D. Binosi and J. Papavassiliou, J. Phys. G **30**, 203 (2004).

[40] D. Binosi and J. Papavassiliou, Phys. Rept. **479**, 1 (2009).

[41] J.M. Cornwall, Phys. Rev. D **26**, 1453 (1982).

[42] J.M. Cornwall, arXiv:0911.0024 [hep-ph], these proceedings.

[43] J.D. Jackson and L.B. Okun, Rev. Mod. Phys. **73**, 663 (2001).

[44] A. Cucchieri and T. Mendes, Nucl. Phys. B **471**, 263 (1996).

[45] A. Cucchieri and T. Mendes, Nucl. Phys. Proc. Suppl. **53**, 811 (1997).

[46] A. Cucchieri and T. Mendes, Comput. Phys. Commun. **154**, 1 (2003).

[47] For a definition of convergence matrix see, for example, Y. Saad, *Iterative methods for sparse linear systems*, PWS Publishing Company, Boston, 1996 (files available at http://www-users.cs.umn.edu/ ∼saad/books.html).

[48] A. Sokal, *Monte Carlo Methods in Statistical Mechanics: Foundations and New Algorithms* (file available at www.stat.unc.edu/faculty/cji/Sokal.pdf).

[49] J. Rank, *Thermal Screening Masses in the Standard Model of Strong and Electroweak Interactions*, Ph.D. thesis, Bielefeld University, January 1998 (file available at http://www.physik.uni-bielefeld.de/ theory/e6/publiframe.html).

[50] K. Amemiya and H. Suganuma, Phys. Rev. D **60**, 114509 (1999).

[51] L. von Smekal *et al.*, PoS **LAT2007**, 382 (2007).

[52] J.C.R. Bloch *et al.*, Nucl. Phys. B **687**, 76 (2004).

[53] See for example A. Cucchieri *et al.*, Phys. Rev. D **76**, 114507 (2007).

[54] D.B. Leinweber *et al.*, [UKQCD Collaboration], Phys. Rev. D **60**, 094507 (1999) [Erratum-ibid. D **61**, 079901 (2000)].

[55] A. Cucchieri, T. Mendes, G. Nakamura and E. M. S. Santos, in preparation.

PoS(QCD-TNT09)009